Reference: *Biol. Bull.* **212:** 67–73. (February 2007)

A Novel Crustacean Swimming Stroke: Coordinated Four-Paddled Locomotion in the Cypridoidean Ostracode *Cypridopsis vidua* (Müller)

GENE HUNT[1,*], LISA E. PARK[2], AND MICHAEL LABARBERA[3]

[1]*Committee on Evolutionary Biology, University of Chicago, Chicago, Illinois 60637;* [2]*Department of Geology, The University of Akron, Akron, Ohio 44325-4104; and* [3]*Department of Organismal Biology and Anatomy, University of Chicago, Chicago, Illinois 60637*

Abstract. Despite the diversity and ecological importance of cypridoidean ostracodes, there have been no kinematic studies of how they swim. We used regular and high-speed video of tethered ostracodes to document locomotion in the cypridoidean species *Cypridopsis vidua.* Swimming in this species is drag-based, with thrust provided by both antennulae and antennae. About 15 complete power and recovery strokes occur per second; maximal speeds for the limb tips were about 30 mm/s for the antennulae and 50 mm/s for the antennae. These speeds correspond to Reynolds numbers on the order of 10^{-1} to 10^{0} for the limb tips and 10^{-2} to 10^{-1} for the setae that extend outward from the swimming limbs and provide much of the surface area of the limb. The strokes of the four thrust-producing limbs are coordinated in a manner that seems to be unique among aquatic arthropods. When viewed from the anterior, power strokes are synchronized diagonally: left antennula and right antenna power strokes start at the same time and terminate just as the power strokes for the right antennula and left antenna begin. Because power strokes occur throughout the stroke cycle, swimming in this species is smoothly continuous, without the rapid accelerations and decelerations characteristic of most small aquatic arthropods.

Introduction

The mechanics of swimming in ostracodes has received relatively little attention compared with that of other aquatic microcrustaceans such as copepods (Buskey, 1998; Lenz and Hartline, 1999; Titelman, 2001; Buskey *et al.,* 2002), isopods (Alexander, 1988; Hessler, 1993), branchiopods (Williams, 1994), and cladocerans (Zaret and Kerfoot, 1980; Kirk, 1985; Lagergren *et al.,* 1997). Prior kinematic research on ostracodes has focused on marine pelagic myodocopids whose relatively large size mitigates some of the technical difficulties of studying locomotion in small swimming animals (Lochhead, 1968; Minkina and Pavlova, 1987; Davenport, 1990). These studies have demonstrated that swimming in myodocopid ostracodes is powered by sweeping motions of the antennal exopod, a finding that supports more casual observations (Skögsberg, 1920; Cohen, 1983).

Aside from the myodocopids, the other major group of swimming ostracodes is the Cypridoidea, a mostly freshwater clade within the podocopids. A number of studies have described the swimming behavior of species within this group, but only in general terms (Skögsberg, 1920; Schreiber, 1922; Canon, 1924; Kesling, 1951). For cypridoideans that swim, the morphology of the limbs, and in some cases, direct observations of swimming animals, have suggested that both antennulae and antennae are involved in providing thrust for locomotion (Skögsberg, 1920; Hoff, 1942). Figure 1 illustrates the morphology of these limbs and their position within the ostracode carapace. Despite the ease with which many cypridoideans can be maintained in the laboratory, there have been no detailed studies of the swimming stroke in this diverse and ecologically important group of ostracodes.

Here we document, using regular and high-speed video, the swimming stroke of the cypridoidean ostracode *Cypridopsis vidua* (Müller 1776). This cosmopolitan Holarctic species is highly mobile, nekto-benthic, phytophilous, and well known to be parthenogenetic (Delorme, 1970, 1989; Uiblein *et al.,* 1996). Although the locomotory behavior of

Received 17 February 2006: accepted 31 October 2006.

* To whom correspondence should be addressed, at Department of Paleobiology, National Museum of Natural History, Smithsonian Institution, Washington DC 20013-7012. E-mail: hunte@si.edu

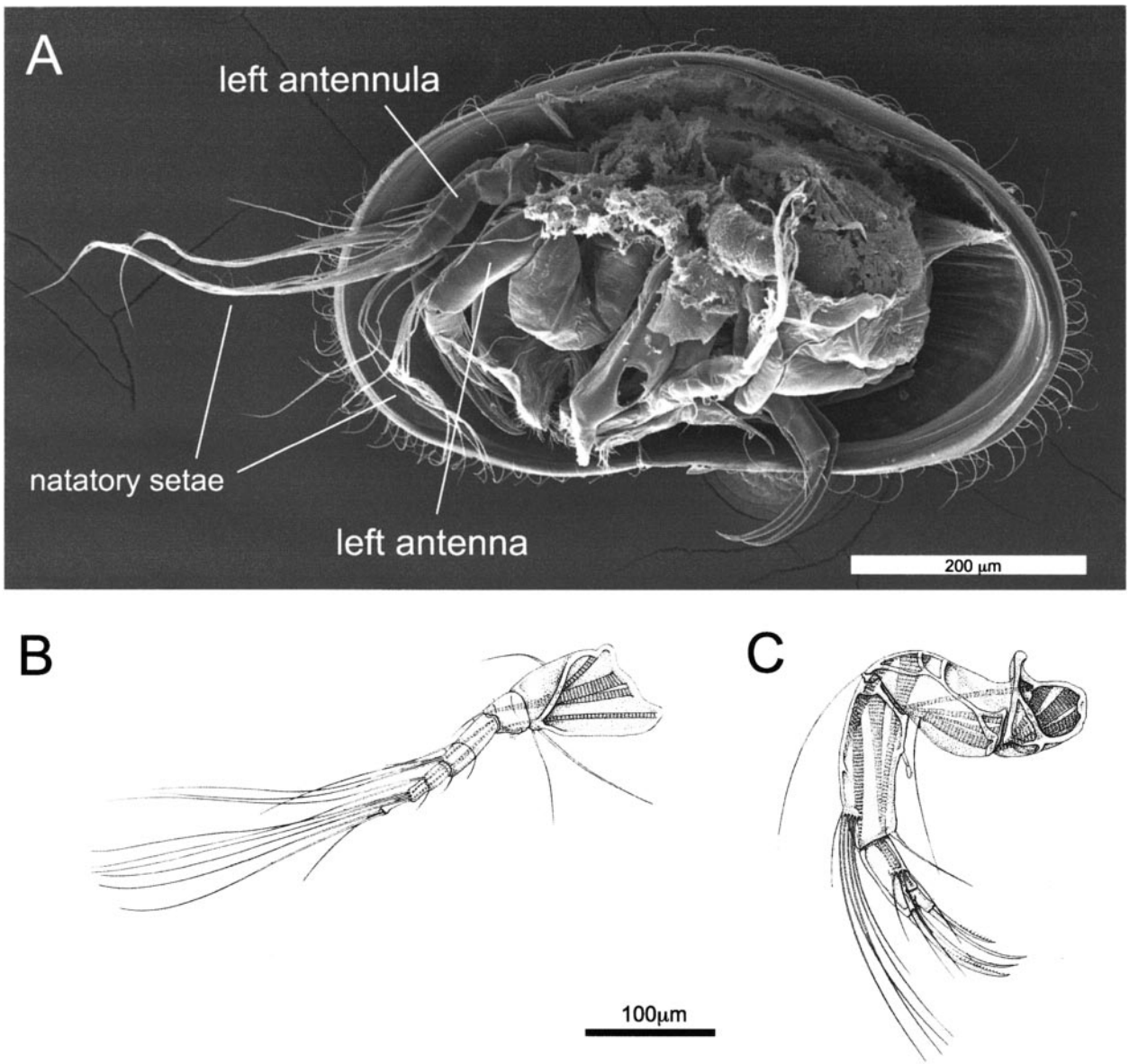

Figure 1. Morphology of *Cypridopsis vidua.* (A) Environmental scanning electron image of critical-point-dried specimen with left valve removed. The anterior of the animal is to the left, and dorsal is toward the top of the page. Drawings of right antennula (B) and right antenna (C), showing natatory setae. Drawings modified from Kesling (1951), with permission from the author.

this species has been studied (Roca *et al.,* 1993; Uiblein *et al.,* 1996), little is known about the mechanics of how these animals swim. Our analyses confirm previous suggestions that both antennulae and antennae power swimming in this species. Moreover, we show that the power strokes of these limbs are coordinated into a four-paddled gait that seems to be unique among aquatic arthropods.

Materials and Methods

A culture of *Cypridopsis vidua* was obtained from a commercial supplier (Ward's Natural Science, Rochester, NY) and maintained in an acrylic plastic container at room temperature. Replacement water from Lake Michigan was added weekly, and boiled wheat grains were added every few weeks as a food source. Specimens of *C. vidua* were observed in their culture container and in a watch glass under a dissecting microscope. In addition, the swimming movements of two tethered and several freely swimming adult specimens were filmed using both regular and high-speed video through a dissecting microscope (Wild M5A). Tethering is common in studies of microinvertebrate swimming because freely mobile animals do not stay in a micro-

scope's field of view long enough to permit detailed observations on limb movements (Hwang *et al.,* 1993). We tethered ostracodes by first using a pipette to remove one from its container and transfer it to a dry microscope slide. Once removed from water, the ostracode tightly closed its valves and remained motionless. A single human eyebrow hair was glued to the end of a 2-mm-diameter wooden dowel for easy manipulation, and the tip of the hair was dipped into a drop of cyanoacrylate (KrazyGlue). The hair was then touched to the lateral side of a valve, where the glue would bond the hair and valve together in a few seconds. The tethered ostracode was then placed under a dissecting microscope in a small water-filled container (≈100 ml) several centimeters from the container's edge. After one to several hours, the ostracode would open its carapace and attempt to swim vigorously. Limb movements were continuous at first, but became increasingly intermittent over the course of a few hours. Resting ostracodes could often be induced to resume swimming by turning off the light source for a few seconds, and then turning it back on. Eventually, the ostracode no longer attempted to swim, presumably due to fatigue or acclimation.

The ostracodes were filmed from several angles, using regular video (30 frames/s [fps]), and high-speed video (250 fps; Redlake MotionScope 1000). About 20 sequences at 30 fps and about 50 at 250 fps were recorded to VHS videotape. This footage was later copied to digital videotape, from which sequences were downloaded for analysis using the software Adobe Premiere (ver. 5.1).

One representative high-speed sequence of 68 frames was selected for detailed analysis. This sequence showed a series of limb motions in lateral view, in which the movements of both right and left antennulae and antennae could be seen. For these frames, the tip and base of all four limbs were digitized in NIH Image (ver. 1.62). From these digitized points, the angle of each limb from the animal's anterior-posterior axis was calculated for each frame in the sequence. We refer to this measure as the stroke angle, which increases as limb tips move posteriorly. The digitized points from the limb tips were smoothed, using the program Quicksand (ver. 008), to reduce digitizing error, and limb speeds were estimated by using the optimally regularized smooth spline algorithm (see Walker, 1998). For a subset of these 68 frames, points were digitized along the length of the right antennula and left antenna to show the position and orientation of the limb segments during the power and recovery strokes.

Results

When tethered and attempting to swim, the ostracode spreads its two valves to allow the movement of limbs. The angle of the gape is about 30° in the anterior region near the antennulae and antennae and about half as wide posteriorly. The position of the swimming limbs in the carapace, along with drawings of these limbs (from Kesling, 1951), is shown in Figure 1. As reported previously, power strokes of both the antennulae and antennae provide thrust for drag-based swimming (Skögsberg, 1920; Schreiber, 1922; Kesling, 1951; *contra* Canon, 1924, who reported that the antennulae were not involved in swimming). The resulting four-paddled locomotion is qualitatively distinct from that of the myodocopid ostracodes that have been studied, all of which rely exclusively on their antennae to power the swimming stroke.

The position and orientation of the right antennula in lateral view during one representative sequence are shown in Figure 2. At the beginning of its power stroke, the antennula is predominantly oriented anteriorward and somewhat dorsally. Through the power stroke, the limb sweeps dorsally and posteriorly, spanning an arc of nearly 90°. The stroke lies within the sagittal plane, with only slight outward movement near the end of the power stroke. The antennula is shown for nine consecutive frames, each 0.004 s apart. During the power stroke, the long setae at the distal end of the antennulae are fully extended in a fanlike configuration (Fig. 1B).

As the power stroke ends and the recovery stroke begins, these long setae collapse from a fan into a tight bundle. The antennula is then pulled close to the carapace by bending at the joints, and the limb moves forward in this "folded" position for about 4–5 frames (0.016–0.020 s, Fig. 2). The entire limb then rotates around the base to return the antennula to its position at the start of the power stroke (Frames 15–17, Fig. 2). Through the 68-frame sequence, each full power and recovery stroke lasts on average about 17 frames (= 0.068 s), which translates into a beat frequency of about 15 cycles/s.

At the beginning of its power stroke, the antenna is located in the anteroventral region of the carapace (Fig. 2). Its power stroke sweeps posteriorly and somewhat ventrally (Fig. 2). As in the antennulae, a group of long setae splay out from the antennae during the power stroke. These antennal setae originate relatively proximally on the limb, at the distal end of the third articulating podomere (Fig. 1C). During the power stroke they form a fanlike splay that follows behind the axis of the limb at an angle of about 30–40°. Because of their relatively proximal placement, these setae increase the effective breadth but not the distal extent of the antennae. As the power stroke slows, the setae collapse against the axis of the antenna, becoming invisible in lateral view.

The orientation of the antenna during the recovery stroke is rather similar to that of the power stroke, but because more of the antenna is pulled inside of the carapace, less is exposed to flow (Fig. 2). The antenna is pulled forward and rotated about the base of the limb located between the valves for about 6 frames (= 0.024 s). Then, the antenna

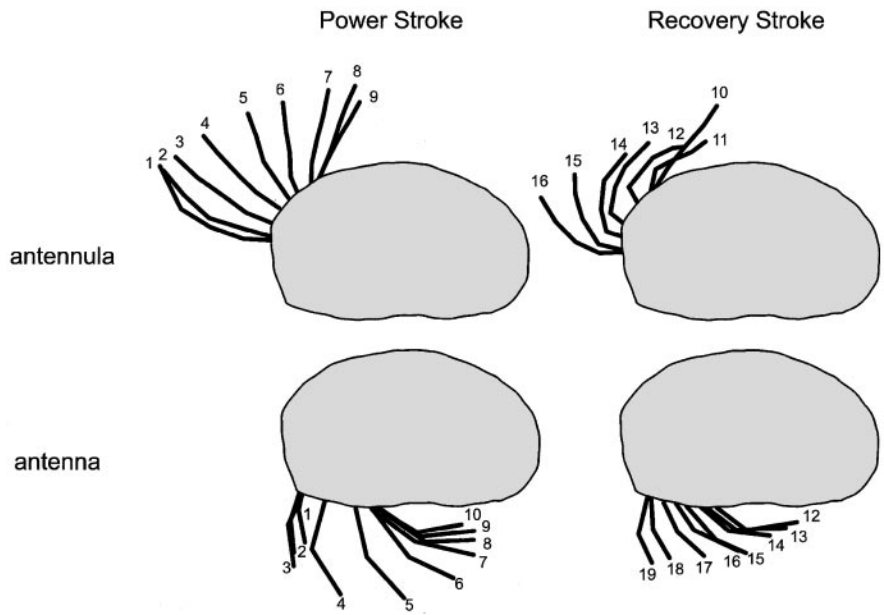

Figure 2. Schematic showing position of right antennula and left antenna in left lateral view during power (left) and recovery (right) strokes. Numbers indicate high-speed video frames, each separated by 0.004 s. Anterior is to the left, and dorsal is toward the top of the page.

moves outward, resuming its initial position at the beginning of the power stroke (Fig. 2, frames 1–3).

During locomotion, the four limbs beat continuously to provide the thrust for swimming. When viewed from the anterior, these four limbs lie in four quadrants with antennulae in the dorsal two quadrants and antennae in the ventral two. Clearly, there are many possible ways to coordinate these four paddles into a swimming stroke, and the manner in which this coordination is accomplished has potential implications for swimming performance.

In this species, the relative timing of limb movements is consistent: power strokes of the left antennula and right antenna are nearly synchronized, as are the strokes of the right antennula and the left antenna. The coordination of limb movements is clear when stroke angles for all four swimming appendages are plotted with respect to time (Fig. 3). As defined here, stroke angle increases during the power stroke and decreases during the recovery stroke. In Figure 3, synchronized (diagonal) limbs are plotted together and are clearly in phase. It can also be seen that the stroke of opposing limb pairs is offset by one-half cycle. For example, the left antennula and right antenna start their coordinated power strokes just as the power strokes of the right antennula and left antenna terminate. Close examination of this plot and of the high-speed sequences revealed that initiation of the antennula power stroke slightly precedes that of its opposite antenna by one or two frames (0.004–0.008 s). This overall pattern of antennula-antenna coordination is very consistent, occurring in all high-speed sequences examined.

Figure 2 suggests that the antennae move considerably faster through the water during the power stroke than during the recovery stroke; the limb travels much farther between frames 4 and 5 than between any successive frames during the recovery stroke (Fig. 2). This impression is supported by direct estimates of the velocity of the distal tip of the limb during swimming. During the power stroke, the antennal tip reaches maximum speeds of about 50 mm/s, about twice the maximum speed measured for the recovery stroke ($\approx$25 mm/s). In contrast, there is almost no difference between maximum speeds during power and recovery strokes of the antennulae; the limb moves with a maximum speed of about 30 mm/s in both directions. Because the terminal podomeres in both limbs have diameters of about 10 μm, these velocities correspond to Reynolds numbers of about 0.3 and 0.5 for the tips of the antennulae and antennae, respectively, during the fastest part of their power strokes. The natatory setae, with diameters of about 2 μm, experience Reynolds numbers of about 0.06 (antennulae) and 0.1 (antennae).

In addition to filming extended sequences of tethered animals, in a few cases we were also able to record freely swimming ostracodes. Although these sequences are generally short because the animals swim out of view within a few strokes, they are sufficient to show that the major features of the swimming stroke that we have described on the basis of tethered animals also appear in freely swimming ones. Thus the movement and coordination of the swimming limbs described here do not appear to be artifacts of tethering (which forces all the energy from the animal's

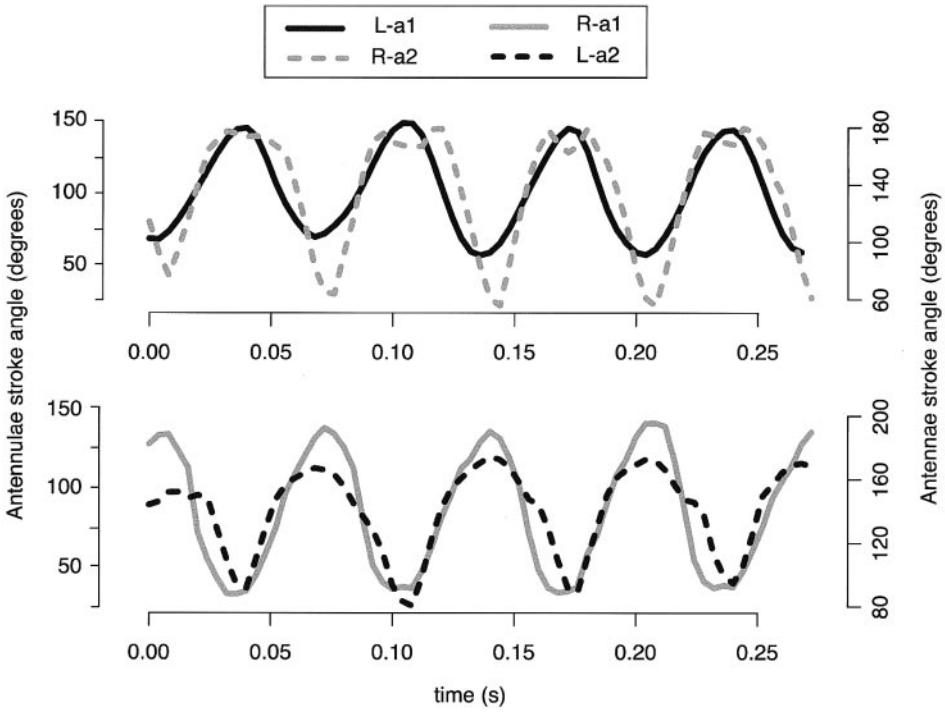

Figure 3. Stroke angle for all four swimming limbs through four complete stroke cycles. Diagonal limbs are plotted together, with left antennula (L-a1) and right antenna (R-a2) in the top panel, and the right antennula (R-a1) and left antenna (L-a2) in the bottom panel. Stroke angle is defined as the angle between the limb axis and the anterior-posterior body axis; stroke angle increases during power strokes and decreases during recovery strokes.

power stroke to go into moving the external fluid rather than producing relative motion between the animal and the fluid; see Emlet and Strathmann, 1985; Emlet, 1990).

Discussion

Cypridopsis vidua, like nearly all small aquatic arthropods, uses setose limbs as oars to provide thrust for swimming. For net forward motion, the total forces exerted against the fluid during each power stroke must exceed the total forces exerted against the fluid during the recovery stroke. This constraint is particularly acute at the relatively low Reynolds numbers that govern swimming in this animal, where drag forces are proportional to wetted area (*i.e.,* total surface exposed to flow, rather than projected area; for a sphere, the wetted area [$4\pi r^2$] is 4 times greater than its projected area) and speed (rather than speed squared) (Vogel, 1994). The swimming stroke in this species exhibits many features commonly employed to ensure that drag during the power stroke exceeds that during the recovery stroke. Important in this regard is the extension of the natatory setae into a broad fan during the power stroke and the collapse of this fan during the recovery stroke. Although difficult to estimate precisely, probably over three-fourths of the surface area of the antennulae and and at least half of the surface area of the antennae is accounted for by the fanlike arrangement of setae. Even though this fan is not a solid surface, closely spaced cylinders behave like a slightly leaky paddle at low Reynolds numbers (Nachtigall, 1980; Koehl, 1995). Moreover, gaps between setae are partially filled in by very fine setules extending from the setae. These setules likely decrease fluid flow between setae, further decreasing the leakiness of the limb as a paddle. During the recovery stroke in both appendages, the setae collapse into a cylindrical bundle and greatly reduce the surface area of the "paddle" relative to the power stroke. This common technique used by many aquatic arthropods to decrease drag during recovery strokes (Vogel, 1994) exploits the fact that drag at low Reynolds number is proportional to the wetted area in contact with the fluid.

Asymmetry in the net forces exerted during the power and recovery strokes is further increased by the change in orientation of the appendages and setae relative to the flow during the swimming cycle. The antennules, antenna, and their setae are all basically cylindrical objects. At low Reynolds numbers, the drag coefficient of a cylinder with its long axis parallel to the flow (as in the recovery stroke) is significantly lower than the drag coefficient of the same cylinder with its long axis perpendicular to the flow (as in

the power stroke); depending on the Reynolds number of the flow and the aspect ratio of the cylinder, the difference may be as great as a factor of 2 (Happel and Brenner, 1991; Vogel, 1994). Thus, during their power strokes, both the antennulae and antennae (and their setae) are in the high drag orientation (perpendicular to relative fluid movement) and switch to a low drag orientation during the recovery stroke.

Another mechanism that increases the asymmetry in net forces between the power and recovery strokes is the tendency for the limbs to remain close to the body of the ostracode during the recovery stroke, rather than fully extended as during the power stroke. In the antennulae this is accomplished by bending at the joints such that the limbs are folded close to the body during the recovery stroke. This same bending occurs in the antennae but to a lesser extent, probably because there are fewer articulating segments than in the antennulae (Fig. 1). In this situation, much of the shear of the fluid (which generates drag forces) occurs between the animal itself (body and valves) and the appendage rather than between the appendage and the surrounding fluid; although energetically expensive, the forces that oppose forward motion of the animal are thus minimized. In addition, the antennae are withdrawn somewhat into the carapace during the recovery stroke, which has the same effect of reducing the limbs' exposure to flow and further minimizing the forces exerted against the bulk fluid (as opposed to against the animal itself).

Because the swimming limbs are diagonally synchronized, there is always a (paired) power stroke occurring while the animal is swimming. As a result, swimming in this species is smoothly continuous, without the large accelerations and decelerations commonly seen in most other microcrustaceans (Zaret and Kerfoot, 1980; Williams, 1994). At the low Reynolds numbers in which these animals function, the dominance of viscous forces disallows effective coasting between power strokes (Williams, 1994).

The observed coordination between limbs probably has advantages over an alternative strategy in which all four limbs start and complete power strokes at the same time. Under a completely synchronized stroke, all four limbs would be in recovery stroke at the same time, causing the animal to come to a complete stop. Thus the mass of the ostracode, and of the water in front of it, would have to be accelerated again with each power stroke. The energetic costs of this acceleration can be substantial relative to locomotion at a constant velocity, even for small crustaceans (Vogel, 1994, p. 365), making this hypothetical stroke less efficient than one in which the animal never stopped completely. There might be specific advantages to coordinating diagonal limbs rather than those on the same side (for example, both antennae, or left antennula and left antenna). The power strokes of each limb produces thrust in nonforward directions—ventral and lateral for the antennulae, and dorsal and lateral for the antennae. Coordinating diagonal limbs may help to cancel out the non-forward thrusts, leading to less wasted lateral movement and more efficient forward motion.

Although the observed limb coordination might have advantages over other conceivable synchronization schemes, it may not be universally optimal or attainable in this group of ostracodes. In fact, we have observed a different, unidentified cypridoidean species in which no power strokes are coordinated. In this species, the power stroke of the left antenna starts halfway through the power stroke of the right antennula, and other limbs' motions are similarly offset by one-quarter of a cycle. Mathematical models, along with comparative study of stroke synchronization and swimming capabilities among cypridoidean ostracodes, should help to elucidate the functional and evolutionary implications of this unusual swimming gait.

Acknowledgments

We thank S. Whittaker of the NMNH SEM facility for preparing specimens and for assistance in SEM imaging, and R. Kesling for permission to reproduce his limb drawings that appear in Figure 1.

Literature Cited

Alexander, D. E. 1988. Kinematics of swimming in two species of *Idotea* (Isopoda: Valvifera). *J. Exp. Biol.* **138:**37–49.

Buskey, E. J. 1998. Energetic costs of swarming behavior for the copepod *Dioithona oculata. Mar. Biol.* **130:**425–431.

Buskey, E. J., P. H. Lenz, and D. K. Hartline. 2002. Escape behavior of planktonic copepods in response to hydrodynamic disturbances: high speed video analysis. *Mar. Ecol. Prog. Ser.* **235:**135–146.

Canon, H. G. 1924. On the feeding mechanism of a freshwater ostracod, *Pionocypris vidua* (O.F. Müller). *Zool. J. Linn. Soc. Lond.* **36:**325–335.

Cohen, A. C. 1983. Rearing and postembryonic development of the myodocopid ostracode *Skogsbergia lerneri* from coral reefs of Belize and the Bahamas. *J. Crustac. Biol.* **3:**235–256.

Davenport, J. 1990. Observations on swimming, posture and buoyancy in the giant oceanic ostracods, *Gigantocypris mulleri* and *Macrocypridina castanea. J. Mar. Biol. Assoc. UK* **70:**43–55.

Delorme, L. D. 1970. Freshwater ostracodes of Canada, part 2: subfamily Cypridopsinae and Herpetocypridinae, and family Cyclocyprididae. *Can. J. Zool.* **48:**253–266.

Delorme, L.D. 1989. Methods in Quaternary ecology #7: freshwater ostracodes. *Geosci. Can.* **16:**85–90.

Emlet, R. B. 1990. Flow fields around ciliated larvae: effects of natural and artificial tethers. *Mar. Ecol. Prog. Ser.* **63:**211–225.

Emlet, R. B., and R. R. Strathmann. 1985. Gravity, drag, and feeding currents of small zooplankton. *Science* **228:**1016–1017.

Happel, J., and H. Brenner. 1991. *Low Reynolds Number Hydrodynamics.* Kluwer Academic Publishers, Dordrecht, The Netherlands.

Hessler, R. R. 1993. Swimming morphology in *Eurycope cornuta* (Isopoda: Asellota). *J. Crustac. Biol.* **13:**667–674.

Hoff, C. C. 1942. The ostracods of Illinois—their biology and taxonomy. *Ill. Biol. Monogr.* **19:**1–196.

Hwang, J.-S., J. T. Turner, J. H. Costello, D. J. Coughlin, and J. R. Strickler. 1993. A cinematographic comparison of behavior by the

calanoid copepod *Centropages hamatus* Lilljeborg: tethered *versus* free-swimming animals. *J. Exp. Mar. Biol. Ecol.* **167:**277–288.

Kesling, R. V. 1951. The morphology of ostracod molt stages. *Ill. Biol. Monogr.* **21:**1– 324.

Kirk, K. L. 1985. Water flows produced by *Daphnia* and *Diaptomus:* implications for prey selection by mechanosensory predators. *Limnol. Oceanogr.* **30:**679–686.

Koehl, M. A. R. 1995. Fluid flow through hair-bearing appendages: feeding, smelling and swimming at low and intermediate Reynolds numbers. Pp. 157–182 in *Biological Fluid Dynamics,* C. P. Ellington and T. J. Pedley, eds. The Company of Biologists, Cambridge.

Lagergren, R., M. Hellsten, and J. A. E. Stenson. 1997. Increased drag, and thus lowered speed: a cost for morphological defence in *Bosmina (Eubosmina)* (Crustacea: Cladocera). *Funct. Ecol.* **11:**484–488.

Lenz, P. H., and D. K. Hartline. 1999. Reaction times and force production during escape behavior of a calanoid copepod, *Undinula vulgaris. Mar. Biol.* **133:**249–258.

Lochhead, J. H. 1968. The feeding and swimming of *Conchoecia* (Crustacea, Ostracoda). *Biol. Bull.* **134:**456–464.

Minkina, N. I., and E. V. Pavlova. 1987. Swimming rate of *Cypridina serrata* Müller (Ostracoda) in plankton of the Indian Ocean. *Pol. Arch. Hydrobiol.* **34:**309–319.

Nachtigall, W. 1980. Mechanics of swimming in water-beetles. Pp. 107–124 in *Aspects of Animal Movement,* H. Y. Elder and E. R. Trueman, eds. Cambridge University Press, Cambridge.

Roca, J. R., A. Baltanás, and F. Uiblein. 1993. Adaptive responses in *Cypridopsis vidua* (Crustacea: Ostracoda) to food and shelter offered by a macrophyte. *Hydrobiologia* **262:**127–131.

Schreiber, E. 1922. Beiträge zur Kenntnis der Morphologie, Entwicklung und Lebenweise der Süβwasser-Ostracoden. *Zool. Jahrb. Abt. Anat. Ontogenie Tiere* **43:**485– 583.

Skögsberg, T. 1920. Studies on marine ostracods. *Zool. Bidr. Upps. Suppl. 1:*1–782.

Titelman, J. 2001. Swimming and escape behavior of copepod nauplii: implications for predator-prey interactions among copepods. *Mar. Ecol. Prog. Ser.* **213:**203–213.

Uiblein, F., J. R. Roca, A. Baltanás, and D. Danielopol. 1996. Tradeoff between foraging and antipredator behaviour in a macrophyte dwelling ostracod. *Arch. Hydrobiol.* **137:**119–133.

Vogel, S. 1994. *Life in Moving Fluids.* Princeton University Press, Princeton, NJ.

Walker, J. A. 1998. Estimating velocities and accelerations of animal locomotion: a simulation experiment comparing numerical algorithms. *J. Exp. Biol.* **201:**981–995.

Williams, T. A. 1994. A model of rowing propulsion and the ontogeny of locomotion in *Artemia* larvae. *Biol. Bull.* **187:**164–173.

Zaret, R. E., and W. C. Kerfoot. 1980. The shape and swimming technique of *Bosmina longirostris. Limnol. Oceanogr.* **25:**126–133.